Supplementary materials

Flexible Metal-Templated Fabrication of Mesoporous Onion-Like Carbon and Fe_2O_3@N-Doped Carbon Foam for Electrochemical Energy Storage

Jing Li [a, b], Ning Wang *[, b, c], Jie Deng [d], Weizhong Qian *[, b], Wei Chu *[, a]

[a] *Department of Chemical Engineering & Institute of New Energy and Low-carbon Technology, Sichuan University，Chengdu 610065, China*

[b] *Beijing Key Laboratory of Green Chemical Reaction Engineering and Technology, Department of Chemical Engineering, Tsinghua University, Beijing 100084, China*

[c] *Physical Sciences and Engineering Division (PSE), King Abdullah University of Science and Technology (KAUST), Thuwal 23955-6900, Saudi Arabia*

[d] *College of pharmacy and biological engineering, chengdu university, Chengdu 610106, China*

* Corresponding author at: Department of Chemical Engineering & Institute of New Energy and Low-carbon Technology, Sichuan University, Chengdu 610065, China

E-mail address: ning.wang.1@kaust.edu.sa (Ning Wang); chuwei1965@scu.edu.cn (Wei Chu); qianwz@tsinghua.edu.cn (Weizhong Qian).

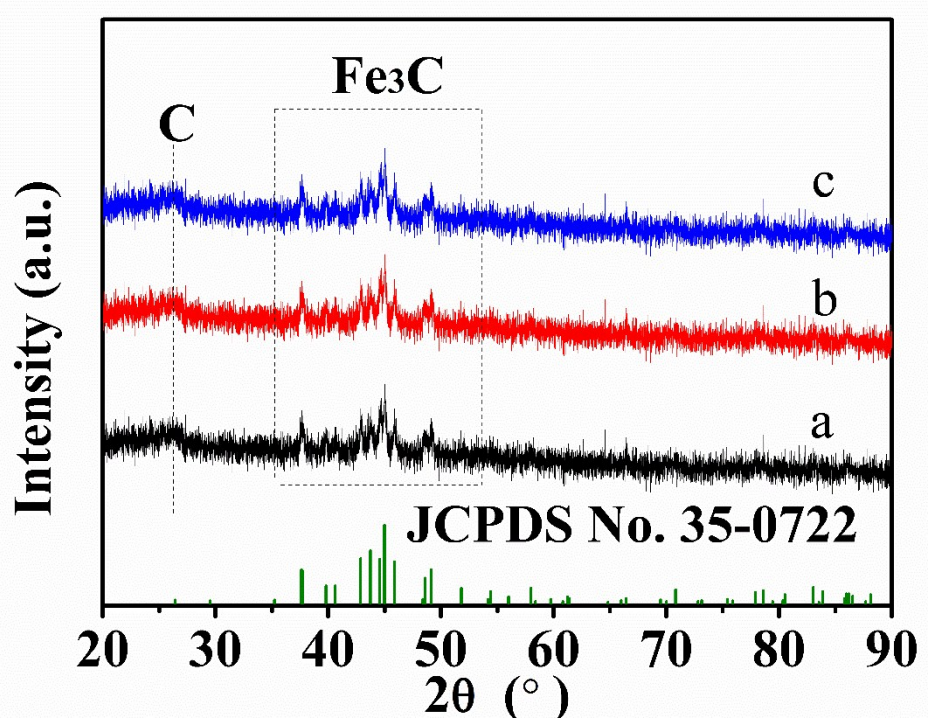

Fig. S1 XRD patterns of Fe_3C@carbon composites precursors for (a) OLC-1, (b) OLC-2, (c) OLC-3, before acid washing.

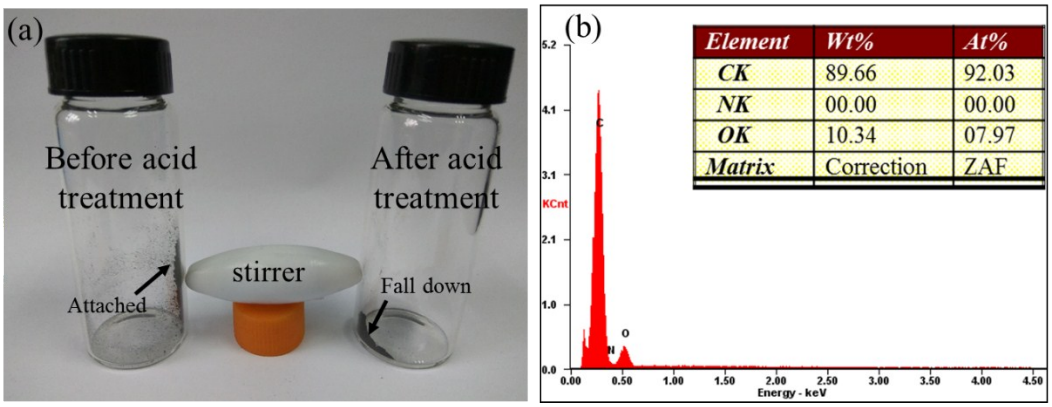

Fig. S2 (a) magnetic test of the sample before (left) and after (right) acid treatment, and (b) EDS result of OLC-3.

Samples	Pore volume ($cm^3\ g^{-1}$)			Specific surface area ($m^2\ g^{-1}$)		
	V_{total}[a]	V_{meso-}	V_{micro-}[b]	S_{total}[c]	S_{meso-}	S_{micro-}[b]
OLC-1	0.536	0.520	0.016	388.9	351.0	37.9
OLC-2	0.431	0.417	0.014	397.0	362.2	34.8
OLC-3	0.335	0.284	0.051	418.2	303.7	114.5

Table S1 N_2 desorption results for OLC-1, OLC-2 and OLC-3.

[a] Calculated by DFT method; [b] Calculated by t-plot method; [c] Calculated by BET method

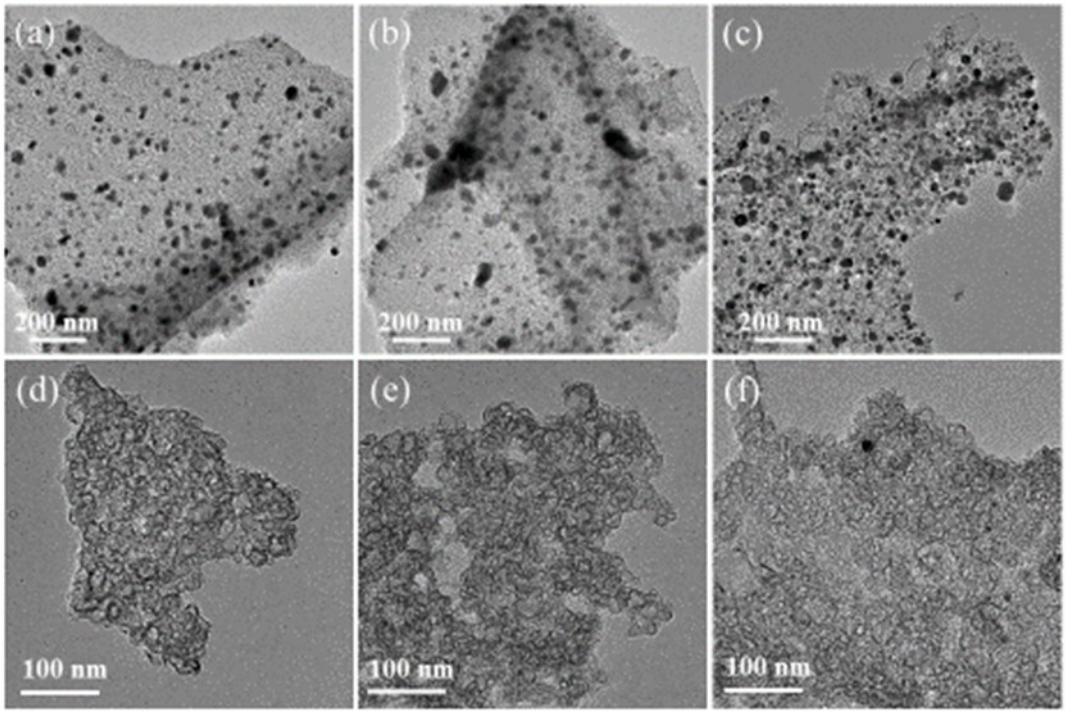

Fig. S3 (a-c) TEM images for Fe_3C@carbon composites precursors for OLC-1, OLC-2, and OLC-3, (d-f) TEM images for OLC-1, OLC-2, and OLC-3, respectively.

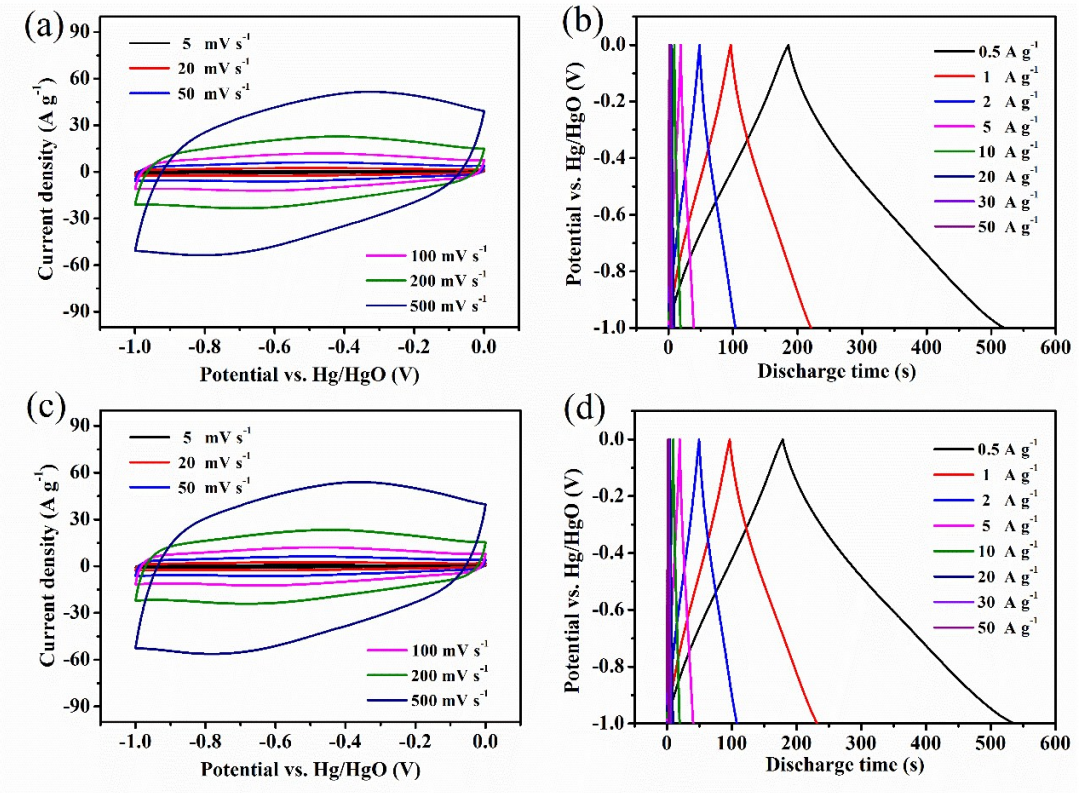

Fig. S4 (a, c) CV curves and (b, d) CD curves for OLC-1 and OLC-2.

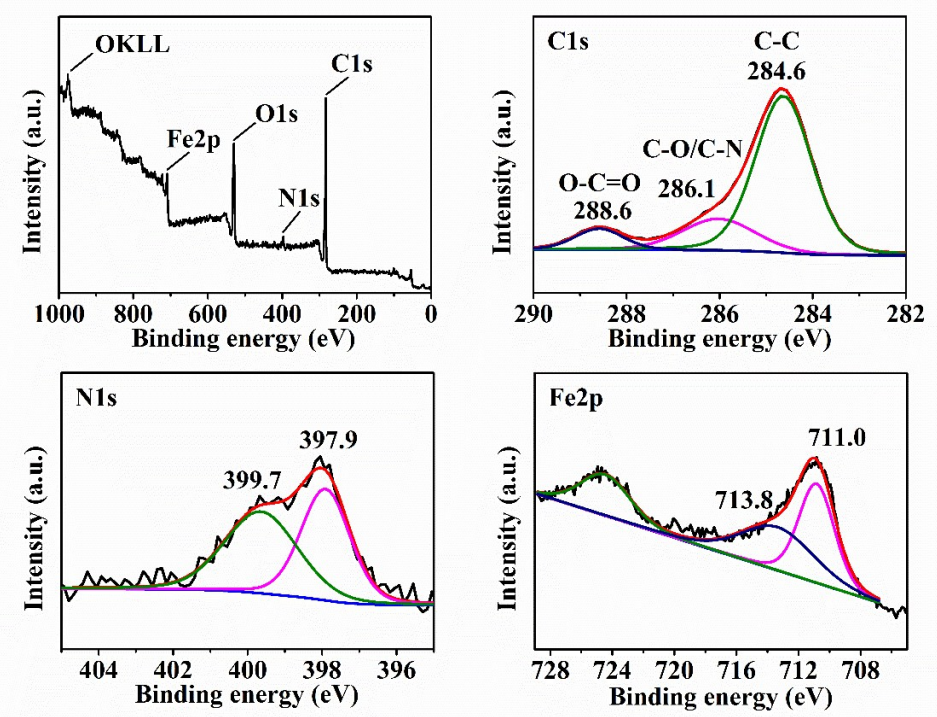

Fig. S5 XPS spectra for Fe_2O_3@NC-2.

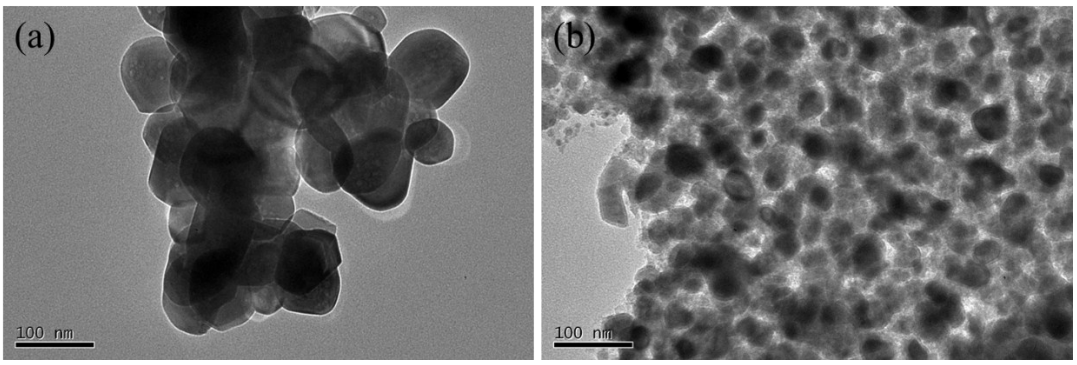

Fig. S6 TEM images for (a) bare Fe_2O_3, and (b) Fe_2O_3@NC-2

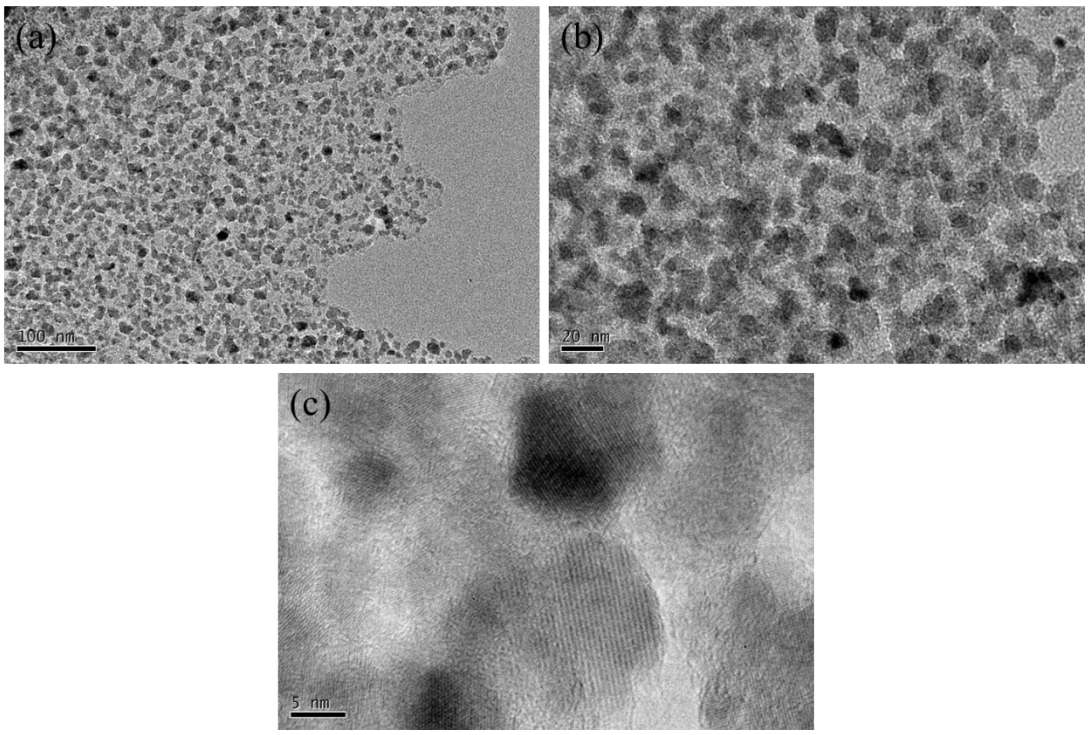

Fig. S7 TEM images for Fe_2O_3@NC-1.5

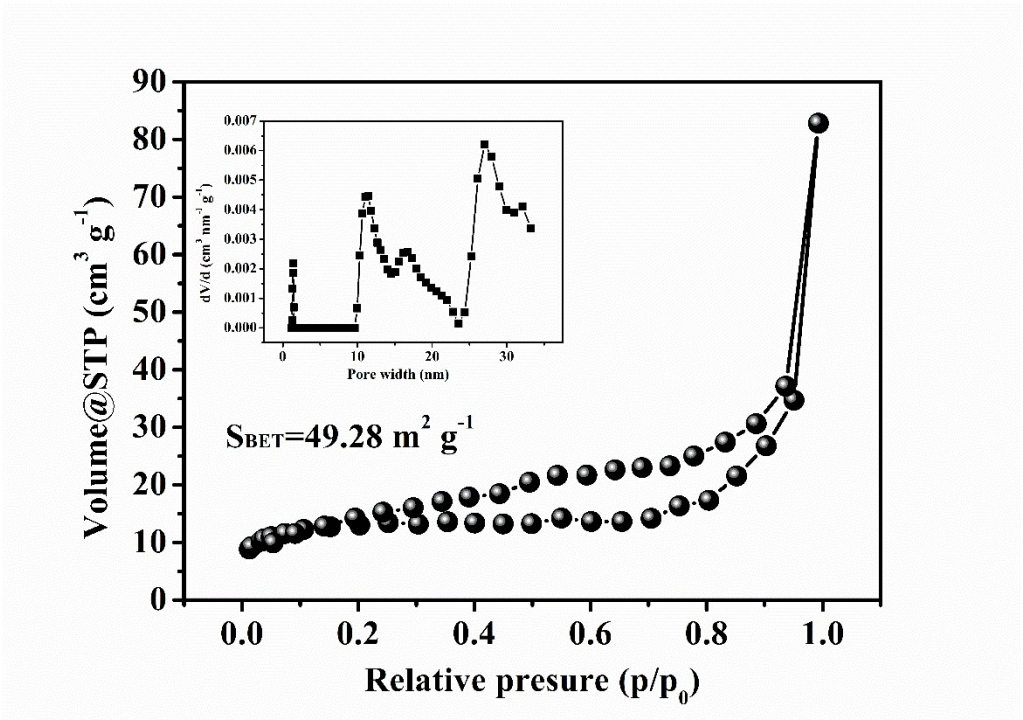

Fig. S8 Specific surface area and pore size distribution of Fe_2O_3@NC-2.

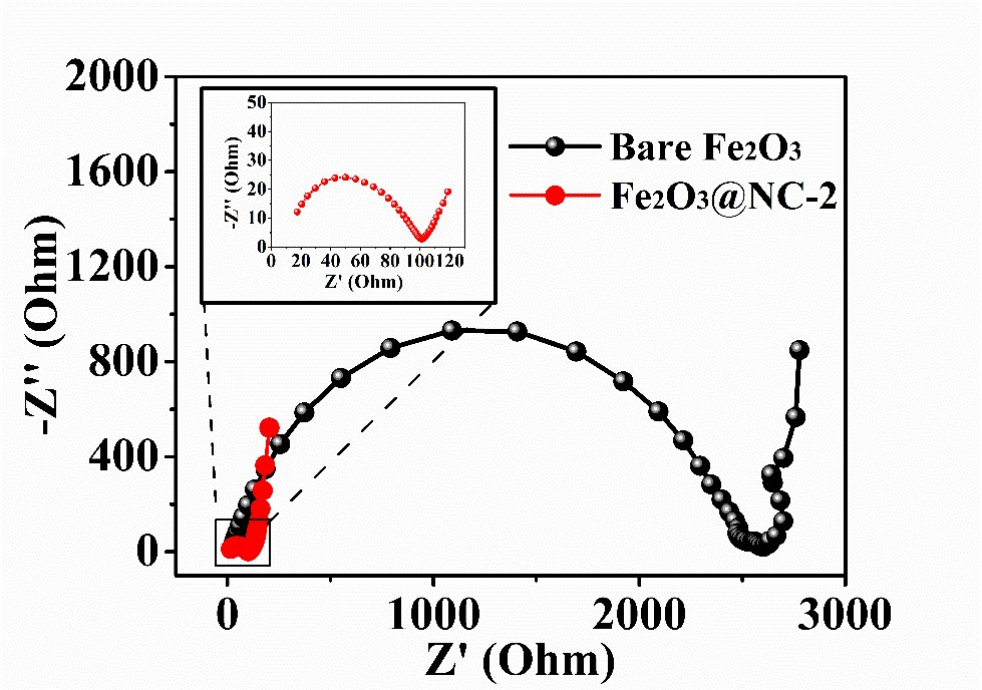

Fig. S9 Nyquist plots for bare Fe_2O_3 and Fe_2O_3@NC-2

Table S2 The electrochemical performance of Fe_2O_3@NC-2 compared with recent literatures.

Samples	Rate capability (mA h g^{-1})		Stability				
			Current density	Cycle number	Initial (mA h g^{-1})	Final (mA h g^{-1})	Fading per cycle (mA h g^{-1})
SnO_2@Fe_2O_3 SNCs [1]	1240.4 (0.1 A g^{-1})	570.7 (1 A g^{-1})	0.5 A g^{-1}	100	848.9	750.8	0.98
N-Fe_2O_3@Carbon [2]	858 (0.1 C)	340 (2 C)	0.1 C	30	923	~800	4.10
MWCNT/γ-Fe_2O_3 [3]	822 (0.05 A g^{-1})	594.3 (1 A g^{-1})	0.1 A g^{-1}	310	-	-	-
Fe_3O_4-Fe@BCNT-34 [4]	813 (0.1 A g^{-1})	434 (2 A g^{-1})	0.3 A g^{-1}	100	694.6	764.1	-
Fe_2O_3/SnO_2 [5]	-	287.3 (2 A g^{-1})	0.2 A g^{-1}	150	1481.6	620.8	5.74
triple-shelled Fe_2O_3 [6]	1186.1 (0.2 A g^{-1})	628.7 (5 A g^{-1})	1 A g^{-1}	200	1085.3	997.8	0.44
UNF–Fe_2O_3 [7]	~1100 (0.1 A g^{-1})	599 (5 A g^{-1})	5 A g^{-1}	500	578	~400	0.36
mesoporous Fe_2O_3 [8]	1286 (0.1 A g^{-1})	~450 (1 A g^{-1})	1 A g^{-1}	230	~1200	420	3.39
Fe_2O_3/CNT–GF [9]	900 (0.2 A g^{-1})	450 (3 A g^{-1})	0.2 A g^{-1}	300	-	> 1000	-
Fe_2O_3@NC-2 (This work)	**735.9** [a] **(0.1 A g^{-1})**	**480.6** [a] **(2 A g^{-1})**	**1 A g^{-1}**	**500**	**566.3** [b]	**372.0**	**0.39**

[a] average reversible discharge capacity calculated by every 10 cycle except for the first discharge capacity.

[b] calculated based on the first 5 cycles except for the first discharge capacity.

- not available

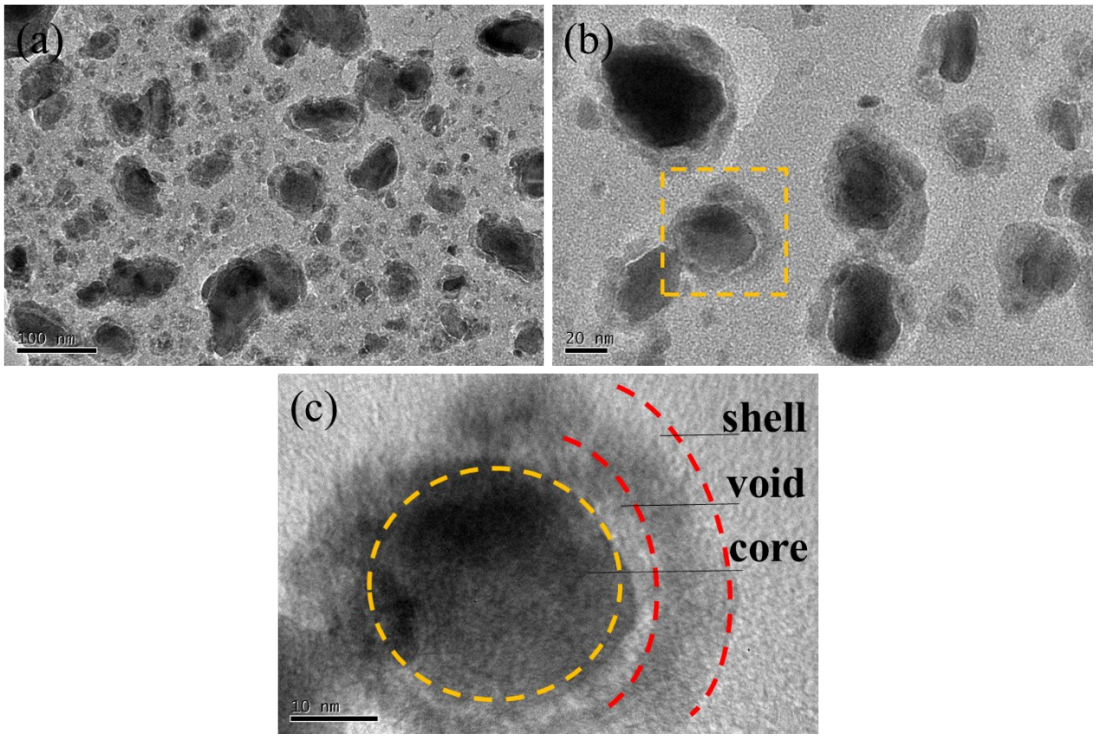

Fig. S10 TEM images of Fe_2O_3@NC-2 after the 500-times cycling test.

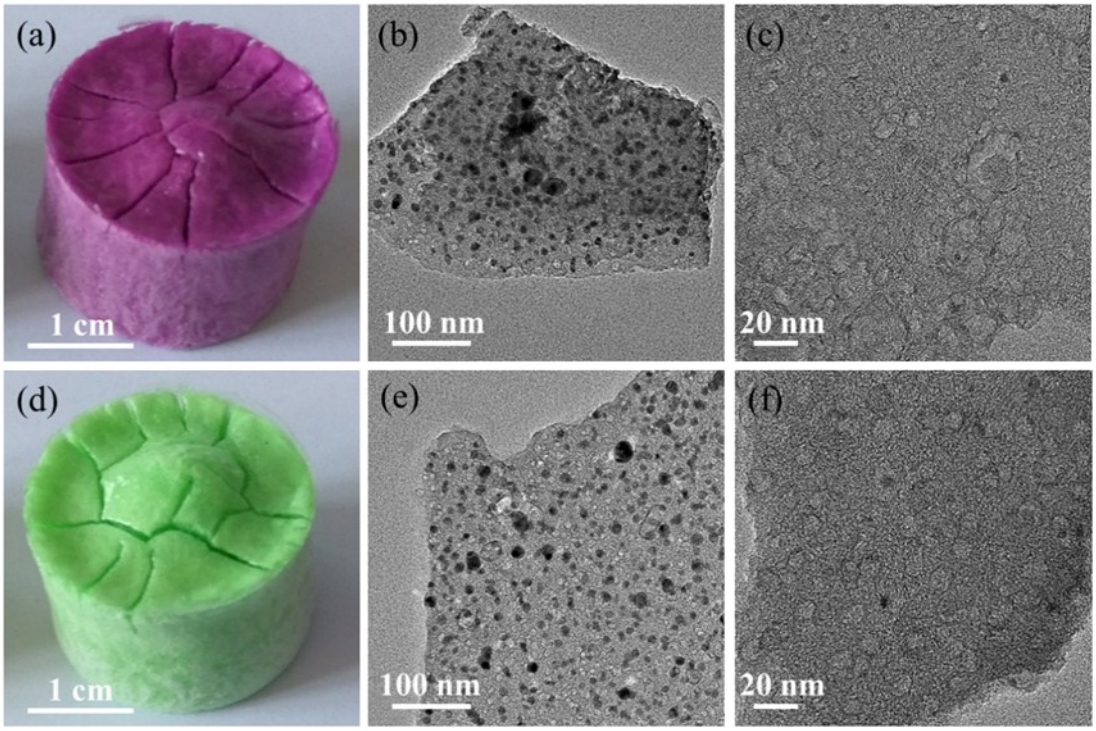

Fig. S11 (a, d) Optical photograph of Co-gelatin and Ni-gelatin aerogel precursors; (b, d) TEM images after heat treatment; (c, f) TEM images after acid leaching.

References:

[1] Y. Zeng, J. Luo, Y. Wang, L. Qiao, B. Zou and W. Zheng, *Nanoscale*, 2017, **9**, 17576-17584.

[2] Y. Yan, H. Tang, F. Wu, Z. Xie, S. Xu, D. Qu, R. Wang, F. Wu, M. Pan and D. Qu, *Electrochimica Acta*, 2017, **253**, 104-113.

[3] P. Bhattacharya, M. Kota, D. H. Suh, K. C. Roh and H. S. Park, *Advanced Energy Materials*, 2017, **7**.

[4] L. Du, C. Xu, J. Liu, Y. Lan and P. Chen, *Nanoscale*, 2017, **9**, 14376-14384.

[5] C. Gu, W. Guan, J.-J. Shim, Z. Fang and J. Huang, *Crystengcomm*, 2017, **19**, 708-715.

[6] J. Sung, C. Lv, F. Lv, S. Chen, D. Li, Z. Guo, W. Han, D. Yang and S. Guo, *ACS Nano*, 2017, **11**, 6186-6193.

[7] Y. Wang, J. Han, X. Gu, S. Dimitrijev, Y. Hou and S. Zhang, *Journal of Materials Chemistry A*, 2017, **5**, 18737-18743.

[8] J. Zhang, T. Huang, Z. Liu and A. Yu, *Electrochemistry Communications*, 2013, **29**, 17-20.

[9] M. Chen, J. Liu, D. Chao, J. Wang, J. Yin, J. Lin, H. Jin Fan and Z. Xiang Shen, *Nano Energy*, 2014, **9**, 364-372.